AIP | Applied Physics Letters

Current induced localized domain wall oscillators in NiFe/Cu/NiFe submicron wires

L. J. Chang, Pang Lin, and S. F. Lee

Citation: Applied Physics Letters **101**, 242404 (2012); doi: 10.1063/1.4770306
View online: http://dx.doi.org/10.1063/1.4770306
View Table of Contents: http://scitation.aip.org/content/aip/journal/apl/101/24?ver=pdfcov
Published by the AIP Publishing

Current induced localized domain wall oscillators in NiFe/Cu/NiFe submicron wires

L. J. Chang,[1] Pang Lin,[1] and S. F. Lee[2,a)]
[1]*Department of Materials Science & Engineering, National Chiao Tung University, Hsinchu 300, Taiwan*
[2]*Institute of Physics, Academia Sinica, Taipei 115, Taiwan*

(Received 26 June 2012; accepted 26 November 2012; published online 10 December 2012)

We experimentally demonstrate domain wall (DW) oscillators excited by in-plane ac current through permalloy based pseudo-spin valve wires, which contain one pair of artificial protrusions. By measuring the spin-transfer-torque induced resonance of a pinned antiparallel transverse DW, under transverse external fields, we show that the antiparallel transverse DW oscillates with a resonance frequency as high as 2.92 GHz, depending on the widths of protrusions. For DW oscillations induced by injection of dc currents, the observed peaks in dV/dI associated with the reversible change of magnetoresistance are attributed to the reversible motions of the DW. © *2012 American Institute of Physics*. [http://dx.doi.org/10.1063/1.4770306]

Dynamics of magnetic domain walls (DW) in ferromagnetic nanowires has undergone intensive theoretical study in view of both fundamental research and the potential for technological applications. Several DW based devices, including spintronic logic[1] and magnetic memory devices,[2,3] have been proposed. In such devices, the DW positions are defined by local pinning sites. These traps consist of structures as artificial notches[4–6] or protrusions[7–9] along a wire. Though notches are usually more effective traps, wires with protrusions are easier to scale down from a fabrication point of view. The DW depinning is preferably achieved by the spin transfer torque exerted by spin polarized currents instead of long-range magnetic fields. In point contact[10–12] or spin valve nanopillar geometry,[13,14] the current is perpendicular to the film plane. The spin transfer torque can compensate the magnetic damping and causes the magnetization to precess at GHz frequencies. Recently, theoretical works on oscillators based on localized steady state DWs driven by spin polarized dc current have been investigated.[15–19] These schemes are very desirable for applications in radio frequency (rf) sources for telecommunications and rf-assisted writing of magnetic bits in recording media.

Numerical simulation studies of the DW oscillator in magnetic nanowires show that when the magnetic field is above the Walker field[3] and below the critical depinning threshold, with the properly chosen magnitude and direction of the in-plane dc current, the velocity of the DW can be tuned to zero. The spatially localized steady state DW oscillator has been generated at finite regions.[16] In soft ferromagnetic nanowires, He and Zhang[15] proposed that the spatially varying damping parameter, via gradient doping of rare earth impurities in the wire, can be employed to control the amplitude and frequency of localized DW oscillations upon the application of a magnetic field and a dc current. Ono and Nakatani[16] suggested that a localized DW oscillation could be induced by injecting dc currents through permalloy wires, and the oscillation could then be converted to a microwave signal by a magnetic tunnel junction. Recent discovery in Ref. 17 reported that DW oscillations could be maintained by the injection of a dc current through a geometrically constrained wire with perpendicular magnetic anisotropy. Moreover, the authors predicted a DW oscillator could work under a low dc current, which excites gigahertz angular precession of a DW at a fixed position with a magnetic anisotropy step created by ion irradiation.[18] Martinez *et al.*[19] analyzed an oscillator based on pinned DWs excited by dc current in a magnetic nanowire of high perpendicular magnetocrystalline anisotropy with the constriction of a square-shaped notch. In accordance with the results of theoretical reports, the resonance frequency was also obtained in the gigahertz level for the pinned DW as a function of ac current frequency.[20–22] However, a report of an experimental result is missing. The fabrication of such devices from prediction of theory is particularly hard due to the needed narrow wire width, leading to cumbersome experimental schemes.

In this paper, we study, experimentally, the localized steady state DW oscillator driven by spin-polarized ac current. The DW was created and pinned at the artificial symmetric protrusion in a NiFe/Cu/NiFe spin valve submicron wire by application of a transverse magnetic field and was then returned to the remnant state. A transverse field was needed in the dc current case for observing the DW oscillation signature. Analysis was made and compared with micro-magnetic simulations to understand the underlying mechanism of the resonance frequency and the observed dV/dI peaks.

Submicron wires were fabricated by electron beam lithography and lift-off process on Si substrates. Our sample wires consist of a spin valve structure, NiFe(24 nm)/Cu(12 nm)/NiFe(12 nm), and their widths are fixed at 400 nm. The length of the wires is 30 μm with a DW trap of one artificial symmetric pair of protrusions halfway along the wires. Fig. 1(a) shows a scanning electron microscopy image of a sample and the schematic measurement configuration. The submicron wire has variable single trap widths $w = 200$, 150, or 100 nm, and fixed 50 nm high protrusions on either side of the wire. The ground-signal-ground (GSG) coplanar waveguide with Au/Cu electrode leads having a characteristic impedance of 50 Ω were then fabricated by a

a)Electronic mail: leesf@phys.sinica.edu.tw.

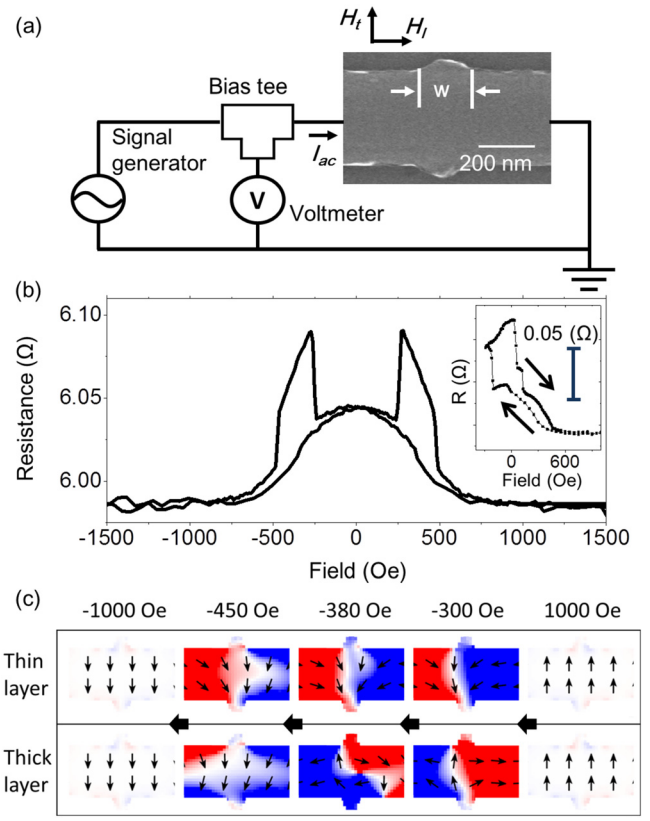

FIG. 1. (a) Schematic diagram of the measurement circuit and a scanning electron microscopy image of a single trap with a 150 nm width, the height of the protrusions is 50 nm on either side of the wire. (b) Experimental magnetoresistance curves of the sample in (a) with an applied transverse field H_t. Inset in (b): Minor MR hysteresis loop. The black arrows show the direction of the field sweep. (c) Simulated magnetic configurations of the thin and thick NiFe layers in the sample with w = 150 nm at various fields.

second lift-off process for resistance measurements. The in-plane external magnetic field H_t was applied transverse to the wire to nucleate the DW in the trap. The oscillation of the DW trapped around the protrusion was excited by injecting an in-plane radiofrequency current I_{ac} along the nanowires, and the resulting dc voltage V_{dc} is synchronously obtained through a bias tee via the electrical contact probe. This DW oscillation produced a time dependent resistance ΔR from the giant magnetoresistance (MR) effect.[23] If the ac current is passed across the DW at resonance frequency f_r, the resistance reaches a maximum due to the coherent DW oscillation.[24,25]

We compared our measurement results with the micromagnetic simulation, in which a unit cell of $5 \times 5 \times 3$ nm^3 and default values of material parameters for $Ni_{80}Fe_{20}$ were used, which are $M_S = 8.0 \times 10^5$ A/m, exchange stiffness constant $A = 1.3 \times 10^{-11}$ J/m, damping parameter $\alpha = 0.01$, and current polarization P = 0.4. The spin polarized current simulations were carried out by numerically solving the Landau-Lifshitz-Gilbert equation with a spin momentum term.[26]

In Fig. 1(b), we present the experimental MR results when the transverse field H_t was applied to the sample with w = 150 nm. The curve has two stable resistance states. The low and high resistance states represent parallel and antiparallel magnetization configurations of the thin and thick layers between the voltage leads, respectively. The magnetization is saturated at 1000 Oe. Slow increase in the resistance occurs from 600 Oe to 0 Oe due to the contribution of the anisotropic magnetoresistance (AMR) when the field is reduced. A large increase at −190 Oe and a plateau of resistance is seen between −200 Oe and −460 Oe. From −470 Oe, the resistance slowly falls to the saturation magnetization state. To understand the details of the reversal process of the magnetization for the MR curve, we carried out a micromagnetic simulation using the OOMMF code. Fig. 1(c) shows the simulated magnetization configurations of the thin and thick NiFe layers. Starting from saturation at 1000 Oe, both the thin and thick layers are parallel to the field. When the external field is reversed to a negative value, we observed an antiparallel transverse domain wall (TDW) between the thin and thick NiFe layers stabilized by the external field, dipole interaction between the two layers, and the geometric constriction from −200 Oe to −370 Oe. The DWs are pinned at the left side of the trap in this simulation. Experimentally, the position of the DW depends on the details of the sample structures. The inset of Fig. 1(b) shows a minor MR hysteresis loop (+1000 Oe to −300 Oe). It demonstrates that the anti-parallel TDW between the thin and thick NiFe layers can be stabilized in a field range from −300 Oe to +50 Oe. At −380 Oe to −390 Oe, the thick layer shows a vortex domain state. Since the stray field from the thick layer vanishes after the nucleation of the vortex DW, the magnetization of the thin layer is no longer affected by the dipolar interaction from the thick layer. As a result, the width of the TDW in the thin layer becomes wider. Upon changing the field from −400 Oe to −1000 Oe, both the thin and the thick layers show a transition to negative saturation.

Fig. 2(a) shows the resistances as a function of the frequency of ac excitation current for the samples with w = 200, 150, and 100 nm at zero applied field. The field sequence of creating the pinned TDWs, as the minor loop in the inset of Fig. 1(b), consists of saturating samples with $H_t = 1500$ Oe, reversing the field to $H_t = -300$ Oe for the anti-parallel TDW nucleation, after which the field is set to zero. The magnetization configuration corresponds to the state with an antiparallel pinned TDW at the trap as shown in Fig. 1(c) with $H_t = -300$ Oe. We sweep the frequency of the ac current from 0.5 to 5 GHz with a fixed amplitude of $I_{ac} = 3$ mA and measure V_{dc} for $I_{dc} = 20\ \mu$A as a function of frequency. Background signals, measured when saturation magnetic fields are applied as in Fig. 2(b), i.e., without any domain walls, are subtracted in Fig. 2(a). A significant resonance peak is observed in each case, which corresponds to the coherent DW oscillations in the pinning potential. The resonance frequency increases as the width of the protrusion decreases. The resonance peak appears at 1.1 GHz with a bandwidth of 165 MHz for the sample of w = 200 nm. For the case of w = 150 nm, a frequency peak at $f_r = 1.83$ GHz is observed, and the bandwidth is 90 MHz. The narrow protrusion w = 100 nm has a resonance peak at $f_r = 2.92$ GHz and the bandwidth is 110 MHz. The resonance frequencies of the DW oscillation under the influence of spin-polarized current in the NiFe nanowire are around several GHz. Such data are in good qualitative agreement with theoretical calculations described by the Landau-Lifshitz-Gilbert equation with spin-transfer-torque contribution.[16,20,21,27] These data show that the resonance frequencies can be controlled by modulating the width of the

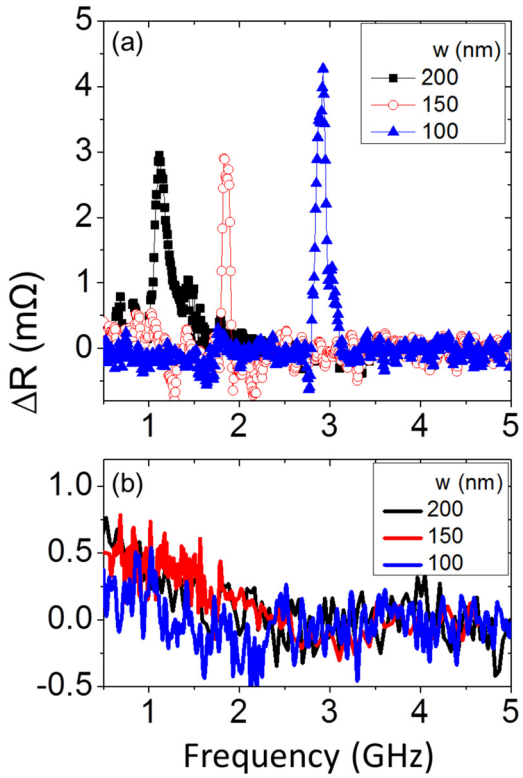

FIG. 2. (a) Experimental measurement of the ac current induces resonance excitation of pinned DW trapped at the protrusion. Resistance change as a function of ac excitation current frequency for the submicron wires containing artificial symmetric protrusions with three different widths of protrusion w = 200, 150, and 100 nm. (b) The response curve measured at the saturation field with a uniform state of submicron wires (without DW). The ΔR is observed unchanged with frequency for each of the samples.

protrusion in a fixed current density. We suggest that the strong restoring force acting on the DW for the narrow protrusion, leading to higher frequency of resonance, is due to the curvature of pinning potential.[28]

Fig. 3(a) shows the dependence on width of the protrusion of the resonance peak by simulation in hollow triangles and experimental data in solid circles. In this simulation, the ac current in the form of $I_{ac}(t) = I_{ac} \sin 2\pi ft$ was applied to excite DW oscillation in the nanowire, where f is the

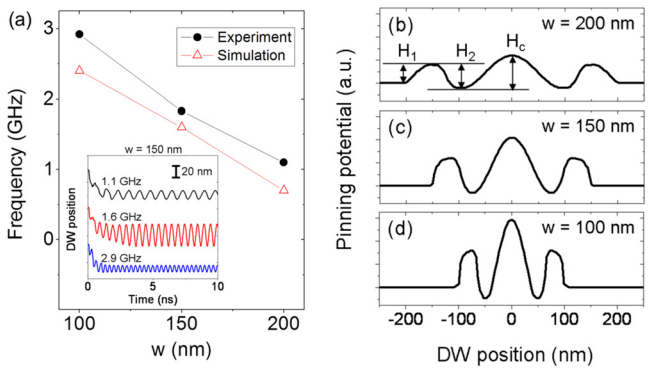

FIG. 3. (a). Resonance frequency of pinned DW dependence on the width of trap w, the solid circles and the open triangles indicate the experiment and simulation results, respectively. The inset shows the simulated time evolutions of the DW motion with w = 150 nm. (b)-(d) Potential landscape of pinned DW from micromagnetic simulation with three different width of protrusion w = 200, 150, and 100 nm.

frequency of the ac current, $I_{ac} = 3$ mA, and t is the time. The resonance frequency is determined from the maximum amplitude of time evolutions of the DW motion[29] as shown in the inset of Fig. 3(a). The solid circles in Fig. 3(a) obtained by measurement are in qualitative agreement with simulation data. The discrepancy could be due to defects or edge roughness in the sample.[30,31] To quantitatively identify the pinning potential profile dependence on the width of the DW trap, micromagnetic simulations (OOMMF) have been used to plot the curve of the potential landscape of our samples. As in the previous study,[7] the potential landscape can be separated into three regimes for the nanowire with a symmetric protrusion, including the side barriers H_1, side wells H_2, and center barrier H_c. The absolute values of H_1, H_2, and H_c increase when the protrusion becomes narrower, as shown in Figs. 3(b)–3(d). We obtained the critical fields with different parameters of the trap from the minor loop technique.[7,32–34] The curvature of the pinning potential can be controlled by changing the width of the protrusion, thereby changing the DW resonance frequency. The higher resonance frequency for the narrow trap is due to the steeper potential landscape, which enhances the restoring force on the pinned DW.[24,35]

We have also performed experiments for the DW resonance frequency as functions of ac current density and the transverse external field. We found the resonance peak is quite stable against small variation of these two parameters. The anti-parallel TDW between the two ferromagnetic layers forms a stable flux closure state to reduce energy because of magnetostatic coupling, while keeping the structure of the pinned DW unchanged. The potential landscape is hardly modulated from the applied current up to our measuring current and magnetic field up to 350 Oe. As a result, the eigenfrequencies for each of the samples were observed.

Since resonant states can be achieved by ac current, we also test whether dc currents can excite trapped DW oscillators. The differential resistance dV/dI with a fixed transverse magnetic field H_t and in-plane dc current of the sample with w = 150 nm is shown for selected values of H_t in Fig. 4(a). All curves display reversible peak structure at different dc current. Similar behavior is also obtained in samples with w = 200 and 100 nm. As shown in the inset of Fig. 4(a), our data show a step of resistance, which is about one tenth of the total MR ratio in Fig. 1(b), and the corresponding peak in dV/dI at $H_t = 210$ Oe. Because this step is reversible with applied current, it is not due to the spin transfer torque induced DW motion propagating through the whole wire. It has been taken as evidence of current induced coherent DW oscillations between the pinned regimes.[36] We plot the critical current I_c corresponding to the peak in dV/dI at different absolute values of the external field H_t from 200 Oe to 460 Oe as shown in Fig. 4(b). The error in I_c, mainly due to uncertainties in geometry, is about 10%. From these results, we defined the boundary for excitation of the DW oscillation by dc current. The critical current varied symmetrically, which is expected from the DW trap with a symmetric potential landscape.[7]

The map of dV/dI versus transverse field and dc current as well as the phase diagram are shown in Figs. 4(b) and 4(c), respectively. These data indicate there are three regions for different behaviors of I_c versus H_t. For region A

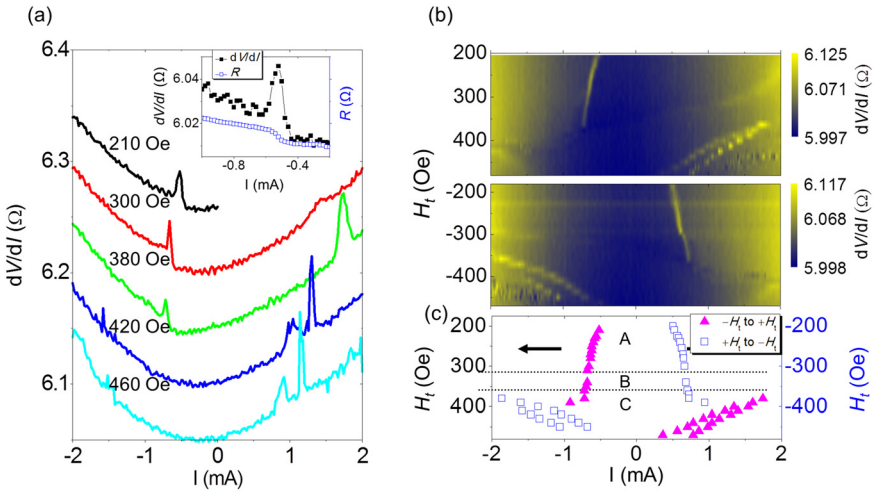

FIG. 4. (a) Differential resistance vs. current density at different external transverse fields H_t, enlarged in the inset for V/I vs. j at $H_t = 210$ Oe. (b) Map of dV/dI versus transverse field and dc current. (c) Critical current I_c vs. H_t.

(anti-parallel TDW), the external field H_t is from 200 Oe to 370 Oe. The I_c slightly increases with increasing H_t. We obtain a linear variation with a small slope. In this situation, there is only one pinned DW oscillator at the trap in the soft NiFe layer responsible for the behavior. The transverse component of DW magnetization and H_t are in the same direction. The DW is slightly wider when H_t is parallel to the wall magnetization. From the theoretical calculation,[37] the value of critical current I_c when the DW starts to oscillate is proportional to the DW width. Our data are consistent with theoretical predictions. Region B is very narrow, 380 Oe $\leqq H_t \leqq$ 390 Oe, where I_c sharply increases in the original current direction. As shown in Fig. 4(a) for $H_t = 380$ Oe, we find another peak appears at the opposite current direction. Simulation results show the nucleation of a vortex DW (VDW) in the hard layer, which is pinned at the right side of the trap for this current and field.

We suggest this new peak is due to a VDW oscillator in the hard NiFe layer induced by dc current at the large transverse field, and the sign of I_c is determined by the VDW pinned location. In region C (parallel TDW) for 400 Oe $\leqq H_t \leqq$ 460 Oe, both peaks sharply decrease with increasing H_t. The peaks of the soft layer are at the opposite current direction. From the results of the simulation, we find the TDW of the soft layer is twisted to the right side of the trap. In this situation, the DW oscillation was necessarily excited by dc current in the opposite direction. Unfortunately, the signal to noise ratio is too small to be resolved on frequency, and time domain measurements for the dc current induces localized DW oscillations. More efforts are needed to obtain direct observations of the dc current induced dynamic of DW oscillators.

We have demonstrated that the DW oscillators can be resonantly excited at the GHz frequency level by in-plane ac current at remnance after an applied transverse field. A strong pinning potential via artificial symmetric protrusions is used to localize the DW, and the oscillation of the wall is simply induced by the injection of in-plane ac current. The well-defined eigenfrequency is dependent on the width of the protrusion. The DW oscillator excited by the injection of in-plane dc current, proposed theoretically in these samples has been studied. We found the boundary for exciting DW oscillation by dc current with a transverse field.

The financial support of the Academia Sinica and the National Science Council of Taiwan, Republic of China are gratefully acknowledged.

[1]D. A. Allwood, G. Xiong, C. C. Faulkner, D. Atkinson, D. Petit, and R. P. Cowburn, Science **309**, 1688 (2005).
[2]M. Hayashi, L. Thomas, R. Moriya, C. Rettner, and S. S. P. Parkin, Science **320**, 209 (2008).
[3]S. S. P. Parkin, M. Hayashi, and L. Thomas, Science **320**, 190 (2008).
[4]M. Hayashi, L. Thomas, C. Rettner, R. Moriya, X. Jiang, and S. S. P. Parkin, Phys. Rev. Lett. **97**, 207205 (2006).
[5]S. Lepadatu, A. Vanhaverbeke, D. Atkinson, R. Allenspach, and C. H. Marrows, Phys. Rev. Lett. **102**, 127203 (2009).
[6]J. Akerman, M. Muñoz, M. Maicas, and J. L. Prieto, Phys. Rev. B **82**, 064426 (2010).
[7]H. T. Zeng, D. Read, D. Petit, A. V. Jausovec, L. O'Brien, E. R. Lewis, and R. P. Cowburn, Appl. Phys. Lett. **94**, 103113 (2009).
[8]E. R. Lewis, D. Petit, L. O'Brien, A.-V. Jausovec, H. T. Zeng, D. E. Read, and R. P. Cowburn, Appl. Phys. Lett. **98**, 042502 (2011).
[9]L. J. Chang, Y. D. Yao, P. Lin, and S. F. Lee, IEEE Trans. Magn. **47**, 2519 (2011).
[10]M. Tsoi, A. G. M. Jansen, J. Bass, W. C. Chiang, M. Seck, V. Tsoi, and P. Wyder, Phys. Rev. Lett. **80**, 4281 (1998).
[11]M. Tsoi, A. G. M. Jansen, J. Bass, W. C. Chiang, V. Tsoi, and P. Wyder, Nature (London) **406**, 46 (2000).
[12]Y. Ji, C. L. Chien, and M. D. Stiles, Phys. Rev. Lett. **90**, 106601 (2003).
[13]S. Urazhdin, N. O. Birge, W. P. Pratt, Jr., and J. Bass, Phys. Rev. Lett. **91**, 146803 (2003).
[14]S. I. Kiselev, J. C. Sankey, I. N. Krivorotov, N. C. Emley, R. J. Schoelkopf, R. A. Buhrman, and D. C. Ralph, Nature(London) **425**, 380 (2003).
[15]J. He and S. Zhang, Appl. Phys. Lett. **90**, 142508 (2007).
[16]T. Ono and Y. Nakatani, Appl. Phys. Express **1**, 061301 (2008).
[17]A. Bisig, L. Heyne, O. Boulle, and M. Kläui, Appl. Phys. Lett. **95**, 162504 (2009).
[18]J. H. Franken, R. Lavrijsen, J. T. Kohlhepp, H. J. M. Swagten, and B. Koopmans, Appl. Phys. Lett. **98**, 102512 (2011).
[19]E. Martinez, L. Torres, and L. Lopez-Diaz, Phys. Rev. B **83**, 174444 (2011).
[20]E. Martinez, L. Lopez-Dias, O. Alejos, and L. Torres, Phys. Rev. B **77**, 144417 (2008).
[21]J. Yoon, C. Y. You, Y. Jo, S. Y. Park, and M. H. Jung, Appl. Phys. Express **4**, 063006 (2011).
[22]J. Yoon, C. Y. You, Y. Jo, S. Y. Park, and M. H. Jung, J. Korean Phys. Soc. **57**, 1594 (2010).
[23]J. C. Sankey, P. M. Braganca, A. G. F. Garcia, I. N. Krivorotov, R. A. Buhrman, and D. C. Ralph, Phys. Rev. Lett. **96**, 227601 (2006).
[24]S. Lepadatu, O. Wessely, A. Vanhaverbeke, R. Allenspach, A. Potenza, H. Marchetto, T. R. Charlton, S. Langridge, S. S. Dhesi, and C. H. Marrows, Phys. Rev. B **81**, 060402 (2010).
[25]C. T. Boone, J. A. Katine, M. Carey, J. R. Childress, X. Cheng, and I. N. Krivorotov, Phys. Rev. Lett. **104**, 097203 (2010).

[26]J. Xiao, A. Zangwill, and M. D. Stiles, Phys. Rev. B **70**, 172405 (2004).
[27]D. V. Berkov, C. T. Boone, and I. N. Krivorotov, Phys. Rev. B **83**, 054420 (2011).
[28]E. Saitoh, H. Miyajima, T. Yamaoka, and G. Tatara, Nature **432**, 203 (2004).
[29]S. Kasai, Y. Nakatani, K. Kobayashi, H. Kohno, and T. Ono, Phys. Rev. Lett. **97**, 107204 (2006).
[30]Y. Nakatani, A. Thiaville, and J. Miltat, Nature Mater. **2**, 521 (2003).
[31]T. W. Chiang, L. J. Chang, C. Yu, S. Y. Huang, D. C. Chen, Y. D. Yao, and S. F. Lee, Appl. Phys. Lett. **97**, 022109 (2010).
[32]D. Petit, A. V. Jausovec, H. T. Zeng, E. Lewis, L. O'Brien, D. Read, and R. P. Cowburn, Phys. Rev. B **79**, 214405 (2009).
[33]L. K. Bogart, D. Atkinson, K. O'Shea, D. McGrouther, and S. McVitie, Phys. Rev. B **79**, 054414 (2009).
[34]D. Petit, A. V. Jausovec, D. Read, and R. P. Cowburn, J. Appl. Phys. **103**, 114307 (2008).
[35]S. Lepadatu, J. S. Claydon, D. Ciudad, C. J. Kinane, S. Langridge, S. S. Dhesi, and C. H. Marrows, Appl. Phys. Lett. **97**, 072507 (2010).
[36]S. Laribi, V. Cros, M. Munoz, J. Grollier, A. Hamzić, and C. D. A. Fert, Appl. Phys. Lett. **90**, 232505 (2007).
[37]G. Tatara and H. Kohno, Phys. Rev. Lett. **92**, 086601 (2004).